NUCLEAR SCIENCE AND ENGINEERING: **179**, 233–252 (2015)

An Improved Resonance Self-Shielding Calculation Method Based on Equivalence Theory

Qian Zhang, Hongchun Wu, Liangzhi Cao,* and Youqi Zheng

Xi'an Jiaotong University, School of Nuclear Science and Technology
Xi'an, Shaanxi, 710049, China

Received December 19, 2013
Accepted May 5, 2014
http://dx.doi.org/10.13182/NSE13-108

Abstract—*The deviation of the effective resonance cross section obtained by conventional equivalence theory for a heterogeneous system is analyzed. It is shown that several approximations commonly adopted in conventional equivalence theory account for the deviation at different levels, with the narrow resonance (NR) approximation being the main source of deviation. Based on the analysis, an improved method based on equivalence theory is proposed. It utilizes the resonance fine flux integral table to minimize the deviation caused by NR approximation. The validity of the method is confirmed by test calculations of effective resonance cross sections in different geometries and different energy group structures. The results of eigenvalue calculations on typical fuel pin cells show that the proposed improvement is effective in reducing the error of infinite multiplication factors of the pin cell. Since the resonance fine flux integral used in this method has already been obtained in calculating the resonance integral table and can be pre-tabulated in the process of generating the library, the implementation of the proposed method is simple and requires no additional calculations. It is useful for improving the accuracy of lattice physics codes based on the equivalence theory.*

I. INTRODUCTION

Resonance self-shielding calculation is one of the key issues in lattice physics computations. The purpose of the resonance self-shielding calculation is to collapse continuous-energy cross sections into multigroup cross sections using the specific neutron spectrum in a homogeneous or heterogeneous system. The specific neutron spectrum weighting of a resonance group needed in the resonance self-shielding calculation is difficult to estimate because of resonance peaks of cross sections within the resonance energy range.

The rigorous approach is to solve the slowing-down equation with ultrafine energy group structure.[1] With sufficient energy discretization, the neutron flux within an energy group is approximately constant. This approach is impractical for complicated geometries because of high computational cost. Another approach, which divides a resonance group into several subgroups according to the magnitude of the cross section within a resonance peak, is called the subgroup method.[2] Since the variation of the cross section in a subgroup is smaller, the neutron flux in a subgroup is approximately constant. The subgroup method is capable of dealing with complicated geometries and has achieved realistic efficiency. However, it is difficult to convert the resonance integral table into appropriate subgroup data with sufficient accuracy and robustness.

The most widely used approach to resonance self-shielding calculation in practical design applications is called equivalence theory. Equivalence theory establishes an equivalent relationship between a heterogeneous system and a homogeneous system by introducing background cross sections.[3–5] The basic calculation procedures are as follows:

1. Effective cross sections or effective resonance integrals of homogeneous cases with different background cross sections and temperature are generated, once and for

*E-mail: caolz@mail.xjtu.edu.cn

all, by an ultrafine-group flux calculator and tabulated in the cross-section library.[6]

2. Background cross sections for resonance regions of the heterogeneous system are evaluated by Dancoff correction[7] or fixed-source transport calculation.[8]

3. Effective cross sections or effective resonance integrals for a desired background cross section and temperature are calculated by interpolation from the resonance integral tables.

The calculation procedure of equivalence theory is of great efficiency and robustness. The theory has been used in lattice physics codes for design applications for many years and historically has a rich validation experience.[9,10] However, there are also crucial limitations to equivalence theory because of the use of approximations. The classical equivalence theory has potential geometrical limitations (e.g., inability to predict a distributed self-shielding effect and to treat complex geometries). However, these limitations can be overcome by improvements (e.g., the spatially dependent Dancoff method,[11] the generalized Stamm'ler method,[12] and the enhanced neutron current method[13]). In spite of the improvements in the treatment of geometry, equivalence theory methods, especially those involving multiterm approximation of escape probability, still suffer from insufficient accuracy in the resolved energy range. Many researchers have proposed empirical corrections to resonance integrals, including a reduction in the ^{238}U resonance integral to achieve good agreement with Monte Carlo *N*-particle transport code results or measured data.[14,15] Some recently proposed equivalence theory methods coupled with the method of characteristics,[16] such as the resonance integral iteration method[8] and the embedded self-shielding method,[17] use resonance integrals of one-dimensional cylindrical geometries instead of homogeneous cases. Some lattice physics codes even partially implement the ultrafine-group slowing-down calculation in the resolved energy range to avoid this problem.[18]

In this paper, to conduct a thorough investigation into the discrepancy caused by the use of equivalence theory, several cases are selected to identify the root reason for the discrepancy, and an improved method is proposed. The structure of the paper is as follows. Section II discusses the validity of effective cross sections obtained by equivalence theory. The discrepancies in the effective cross sections caused by three basic approximations used in the derivation of equivalence theory are evaluated independently. It is shown that the narrow resonance (NR) approximation is the main source of deviation in equivalence theory. Section III proposes a new method with improvements as a countermeasure to the NR approximation and describes the results. Section IV gives a summary and conclusions.

II. DISCREPANCY ANALYSIS IN CONVENTIONAL EQUIVALENCE THEORY

II.A. Equivalence Theory

Consider a simplified two-region problem (fuel and moderator). The fuel region contains one resonance isotope (e.g., ^{238}U). As fission neutrons can be neglected in the resonance region for ^{238}U, the neutron slowing-down equation is

$$\Sigma_{t,f}(E)\phi_f(E)V_f = V_f P_{ff}(E)\int_0^\infty \Sigma_{s,f}(E'\to E)\phi_f(E')\,dE' + V_m P_{mf}(E)\int_0^\infty \Sigma_{s,m}(E'\to E)\phi_m(E')\,dE', \quad (1)$$

where

$\Sigma_{t,f}(E)$ = macroscopic total cross section in fuel

$\Sigma_{s,f}(E'\to E)$, $\Sigma_{s,m}(E'\to E)$ = macroscopic scattering cross sections in fuel and moderator, respectively

$\phi_f(E')$, $\phi_m(E')$ = neutron fluxes in fuel and moderator, respectively

V_f, V_m = volumes of fuel and moderator, respectively

$P_{ff}(E)$, $P_{mf}(E)$ = fuel-to-fuel and moderator-to-fuel collision probabilities, respectively.

The first approximation used in the derivation is the NR approximation. It is based on the assumption that the resonance width is narrow compared with the slowing-down width. This means that neutrons appearing in the resonance peak are from outside the peak, where the neutron spectrum is nearly proportional to $1/E$. Neutron fluxes in Eq. (1) can be written as $1/E$. With the use of the reciprocity theorem, Eq. (1) is simplified to

$$\phi_f(E) = \frac{1}{E}\left[\frac{\Sigma_{pf}}{\Sigma_{tf}(E)}\{1 - P_{fm}(E)\} + P_{fm}(E)\right]. \quad (2)$$

The second approximation is a rational approximation of the escape or collision probability. The rational form is crucial because it achieves the same analytic form for the flux between the heterogeneous and homogeneous systems. Multiterm rational approximation leads to a remarkable improvement in the accuracy of the fuel-to-moderator collision probability. It is given as

$$P_{fm}(E) = \sum_{n=1}^{N}\frac{b_n a_n}{\Sigma_{t,f}(E)\bar{l} + a_n}, \qquad \sum_{n=1}^{N} b_n = 1, \quad (3)$$

where

$\bar{l}$ = average chord length of the fuel lump

b_n, a_n = coefficients of the rational approximation.

The flux in Eq. (2) is then expressed as

$$\phi_f(E)=\frac{1}{E}\sum_{n=1}^{N} b_n \frac{\sigma_{p,r}+\sigma_{0,n}}{\sigma_{t,r}(E)+\sigma_{0,n}},\ \sigma_{0,n}=\sigma_{0,f}+a_n/N_r\bar{l}\ , \quad (4)$$

where

N_r = number density of resonance nuclide r

$\sigma_{p,r}$ = microscopic potential scattering cross section of nuclide r

$\sigma_{0,f} = \sum_{k\neq r} N_k\sigma_p^k \Big/ N_r$

$\sigma_{t,r}$ = microscopic total cross section of resonance nuclide r

$\sigma_{0,n}$ = microscopic background cross section.

Using Eq. (4), the effective microscopic cross section of reaction x is given by

$$\begin{aligned}\sigma_{x,g}&=\frac{\int_{\Delta E_g}\sigma_x(E)\phi_f(E)\,dE}{\int_{\Delta E_g}\phi_f(E)\,dE}\\&=\frac{\int_{\Delta E_g}\sigma_x(E)\frac{1}{E}\sum_{n=1}^{N} b_n\frac{\sigma_{p,r}+\sigma_{0,n}}{\sigma_{t,r}(E)+\sigma_{0,n}}\,dE}{\int_{\Delta E_g}\frac{1}{E}\sum_{n=1}^{N} b_n\frac{\sigma_{p,r}+\sigma_{0,n}}{\sigma_{t,r}(E)+\sigma_{0,n}}\,dE}\\&=\frac{\sum_{n=1}^{N} b_n I_{g,x}(\sigma_{0,n})}{1-\sum_{n=1}^{N} b_n I_{g,a}(\sigma_{0,n})\big/(\sigma_{p,r}+\sigma_{0,n})}\ , \end{aligned} \quad (5)$$

where

$$I_{g,x}(\sigma_{0,n})=\int_{\Delta E_g}\sigma_x(E)\left(\frac{1}{E}\frac{\sigma_{p,r}+\sigma_{0,n}}{\sigma_{t,r}(E)+\sigma_{0,n}}\right)dE\Big/\int_{\Delta E_g}\frac{1}{E}\,dE\ . \quad (6)$$

In this derivation, the resonance integral is calculated using the approximated flux shape in Eq. (6). However, in practice, $I_{g,x}(\sigma_{0,n})$ is the result of interpolation in the resonance integral table using $\sigma_{0,n}$, and the resonance integral table is partially calculated by the ultrafine-group method. In other words, the expression for the flux in Eq. (6) based on the NR approximation is necessary for the derivation to proceed from Eq. (2) to Eq. (4); however, it is not necessary for calculating the resonance integrals. Thus, two meanings can be attributed to "NR approximation" with regard to its effect on the accuracy of equivalence theory, and these two meanings will be discussed in turn in this paper. Equation (5) is the final expression for the effective resonance cross section of a fuel lump in a two-region heterogeneous system. Besides the NR approximation and multiterm rational probability approximation, the two-region fuel-moderator heterogeneous system itself is also an approximation, because a spatially constant macroscopic total cross section of the fuel lump is used in the evaluation of fuel-moderator collision probability. The distributed resonance self-shielding effect within the fuel lump is neglected in the derivation of equivalence theory.

II.B. Discrepancy Analysis

The discrepancy analysis is based on comparison of effective microscopic absorption cross sections generated by equivalence theory and the ultrafine-group slowing-down calculation using several calculation conditions. An ultrafine-group calculation code UFO (Ref. 19) is developed to calculate the slowing-down equation (1) without using the NR approximation. The neutron collision probability in Eq. (3) can be given by both rigorous calculation and multiterm rational approximation. The fuel rod can be subdivided by UFO calculations to consider the distributed resonance self-shielding effect. The calculation conditions are as follows:

1. isolated fuel rod surrounded by infinite moderator H
2. fuel consisting of only ^{238}U with $N_{238} = 0.02\times10^{24}$ atoms/cm^3
3. fuel diameter 1.0 cm ($\bar{l}=1.0$ cm)
4. rational approximation in Eq. (3): Carlvik's two-term rational approximation[7] and a three-term rational approximation calculated by numerical solution
5. resonance integral used in equivalence theory: generated by UFO calculations on a homogeneous system of different N_H/N_{238} compositions
6. energy group structure: WIMS 69-group[20] and XMAS 172-group.[21]

This specific case is studied to narrow down the source of deviation by equivalence theory. In the conventional resonance calculation procedure based on equivalence theory, besides the three approximations mentioned in Sec. II.A, there are other factors affecting the final results of effective cross sections, such as a group-dependent λ factor for intermediate resonance treatment,[22] the resonance overlap effect,[23] Dancoff factor calculation, and the resonance integral interpolation method.[24] Research on these factors is important to

obtain more accurate resonance calculation results. However, these are not essential approximations or assumptions used in the derivation of the final expression for the effective cross section, and they can be avoided under the calculation conditions given above. In contrast, the three basic approximations used in the derivation of equivalence theory cannot be avoided. In this specific case, the moderator is infinite, so the Dancoff factor is 1.0 and the λ factor for H is 1.0. There is only one resonance isotope, ^{238}U, so there is no resonance overlap effect. The resonance integral used is calculated by ultrafine-group slowing-down calculation instead of interpolation in the resonance integral table. The source of the deviation caused by equivalence theory is narrowed down to three basic causes. The main purpose of Secs. II.B.1, II.B.2, and II.B.3 is to determine how much deviation is caused by each of the three basic approximations. The following methods are used to generate the effective cross sections:

1. *method 1:* equivalence theory, neutron collision probability calculated by Carlvik's approximation, two-region approximation
2. *method 2:* equivalence theory, neutron collision probability calculated by the rigorous method, two-region approximation
3. *method 3:* ultrafine-group slowing-down calculation, neutron collision probability calculated by the rigorous method, two-region approximation
4. *method 4:* ultrafine-group slowing-down calculation, neutron collision probability calculated by Carlvik's approximation, two-region approximation
5. *method 5:* ultrafine-group slowing-down calculation, neutron collision probability calculated by the rigorous method, multiregion calculation.

The differences in the infinite multiplication factors caused by the three basic approximations are analyzed in Sec. II.C.

II.B.1. Rational Approximation of Neutron Collision Probability

The rational approximation of the neutron collision probability is crucial in the derivation of equivalence theory because the flux of the heterogeneous system can be expressed in a form similar to that of the flux of the homogeneous system based on this approximation. In the conventional Stamm'ler method, Carlvik's two-term rational approximation in cylindrical geometry is used. To treat more complex geometries with sufficient accuracy, three or more terms of rational approximations have been proposed.[12] For the specific case described in Sec. II.B, we give a three-term rational approximation whose coefficient is calculated by numerical solution. The coefficients are as follows: Carlvik's two-term rational approximation:

$$b_1 = 2,\ b_2 = -1,\ a_1 = 2,\ a_2 = 3\ .$$

Three-term rational approximation by numerical solution:

$$b_1 = 1.513,\ b_2 = 1.169,\ b_3 = -1.682,$$

$$a_1 = 2.109,\ a_2 = 2.106,\ a_3 = 2.766\ .$$

Figure 1 illustrates the absolute differences between the exact values of the neutron escape probability in cylindrical geometry obtained by numerical solution and those calculated by multiterm rational approximations. The result shows that three-term approximation improves the accuracy of escape probabilities. There is still a discrepancy distribution between the reference escape probabilities and the approximate multiterm rational escape probabilities. In reality, the asymptotic behavior of the neutron collision probability when $\Sigma_{t,f} \to \infty$ is exponential, and discrepancy always exists when the rational terms are used to approximate the collision probability.

The derivation of equivalence theory in Sec. II.A shows that the rational approximation of the escape probability is necessary. Since the discrepancy always exists when the rational approximation is used, there is no way to obtain method 2 from the conventional derivation introduced in Sec. II.A. However, in the recent study by Zhang et al.,[25] there is an alternative way to realize the equivalence relationship by a procedure involving integration of reaction rates over the resonance energy domain.

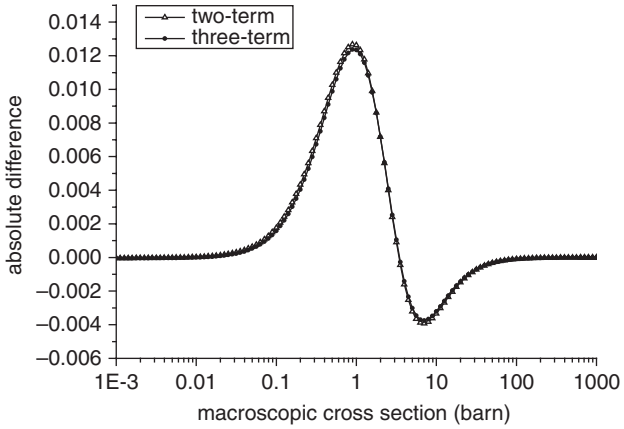

Fig. 1. Absolute difference between reference escape probabilities and approximate multiterm rational escape probabilities.

Without Eq. (3), the reaction rate can be expressed as

$$RI = \int_{\Delta E_g} \sigma_x(E)\phi_f(E)\,dE$$

$$= \int_{\Delta E_g} \sigma_x(E)\frac{1}{E}\left[\frac{\Sigma_{pf}}{\Sigma_{tf}(E)}\{1-P_{fm}(E)\}+P_{fm}(E)\right]dE\,. \quad (7)$$

From the viewpoint of reaction-rate preservation, there is always a specific homogeneous case with background cross section $\sigma_{b,x}$ that can match the reaction rate given by Eq. (7). The following equation is given:

$$\int_{\Delta E_g} \sigma_x(E)\frac{1}{E}\left[\frac{\Sigma_{pf}}{\Sigma_{tf}(E)}\{1-P_{fm}(E)\}+P_{fm}(E)\right]dE$$

$$= \int_{\Delta E_g} \sigma_x(E)\left(\frac{1}{E}\frac{\sigma_{p,r}+\sigma_{b,x}}{\sigma_{t,r}(E)+\sigma_{b,x}}\right)dE\,. \quad (8)$$

Once $P_{fm}(E)$ is given in an ultrafine-group structure, the reaction rate can be calculated by an integration procedure. Equation (8) then becomes an implicit equation in $\sigma_{b,x}$. For each energy group, $\sigma_{b,x}$ can be solved by Newton-Raphson iteration. Finally, $\sigma_{b,x}$ for each group is used for interpolation in the resonance integral table. Once $P_{fm}(E)$ is given in an ultrafine-group structure, no matter in which way the escape probability is calculated, there is a specific homogeneous case with background cross section $\sigma_{b,x}$ that preserves the reaction rate calculated by $P_{fm}(E)$.

Method 1 is the conventional procedure of the Stamm'ler method using the resonance integral calculated by UFO. However, to evaluate the discrepancy caused by rational approximation of the escape probability, both methods 1 and 2 are performed by the alternative way introduced above. Escape probabilities in ultrafine-group structure are calculated by rational approximation in method 1 and by rigorous numerical solution in method 2. Both methods utilize equivalence theory, and the only difference between methods 1 and 2 is the procedure for calculating the neutron collision probability.

The relative difference in microscopic absorption cross sections calculated by methods 1 and 2 is shown in Fig. 2. The results show that the three-term rational approximation is slightly better than Carlvik's two-term approximation and that the maximum difference in the effective cross sections caused by the approximation of probabilities is fairly small: both approximations are $<0.5\%$ using the results of method 2 as reference.

Comparison of effective microscopic cross sections calculated by methods 3 and 4 gives an alternative way to evaluate the difference caused by the approximation of neutron collision probabilities. In methods 1 and 2, Eq. (2) with the NR approximation is used to evaluate the flux. Methods 3 and 4 utilize the ultrafine-group slowing-down procedure to calculate the flux exactly with heterogeneous neutron collision probabilities. The only difference between methods 3 and 4 is the procedure for calculating the neutron collision probability.

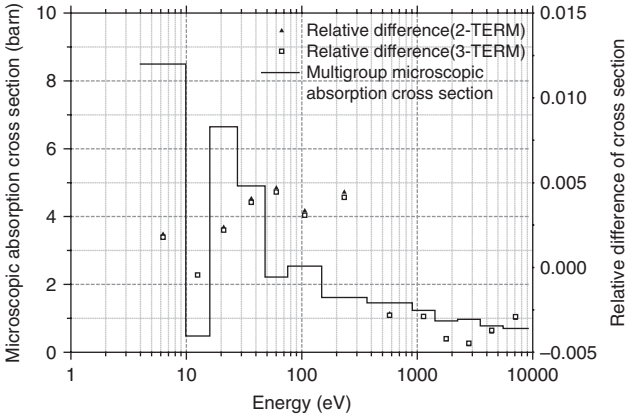

Fig. 2. Relative difference in effective microscopic cross sections (absorption) of ^{238}U calculated by methods 1 and 2, depicted with the reference absorption cross section of ^{238}U (69-group structure).

The relative difference in microscopic absorption cross sections calculated by methods 3 and 4 is shown in Fig. 3. The discrepancy distribution along energy groups is similar to the results in Fig. 2: the three-term approximation gives slightly better results, and the maximum relative differences caused by two- and three-term approximations are both $<0.5\%$ using the results of method 3 as reference.

The three-term approximation gives a significant improvement when predicting the escape probability for a complex geometry. However, in this case, which contains

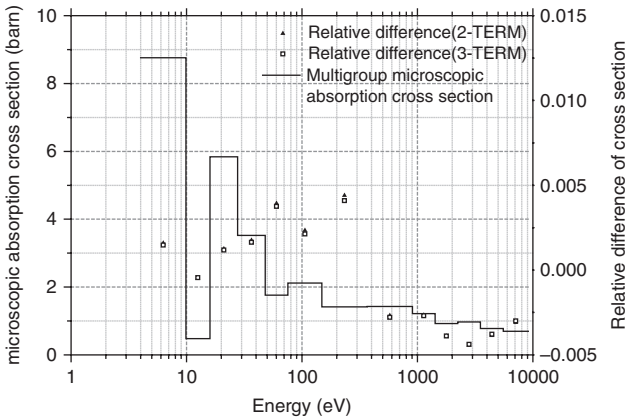

Fig. 3. Relative difference in effective microscopic cross sections (absorption) of ^{238}U calculated by methods 3 and 4, depicted with the reference absorption cross section of ^{238}U (69-group structure).

an isolated fuel rod surrounded by infinite moderator, both Carlvik's two-term rational approximation and the three-term approximation achieve good accuracy. In this case, the comparisons using the calculation procedures of both equivalence theory (preserving the reaction rate) and the ultrafine-group method show that the three-term approximation gives a slightly better improvement than the two-term rational approximation and that the results of both the two- and three-term approximations are close to the results with rigorous probabilities.

The results show that Carlvik's two-term rational approximation is sufficiently accurate for an isolated fuel cell. This conclusion is not in conflict with the results of previous studies (e.g., Ref. 10). Although the three-term approximation improves the accuracy of the escape probability, in this case, it does not lead to a considerable correction. Even using rigorous probabilities, the correction to the effective cross section is still $<0.5\%$. Compared with what will be seen in the following discussion of other approximations and the analysis of infinite multiplication factors, Carlvik's two-term rational approximation of neutron collision probabilities is not the main source of deviation in the effective cross section.

II.B.2. Two-Region Fuel-Moderator Heterogeneous System Approximation

In the evaluation of the escape probability from the fuel rod, the total cross section in the rod is assumed to be spatially constant. Because of the spatially dependent flux distribution in the rod, the resonance cross sections of ^{238}U are spatially dependent. The distributed microscopic absorption cross sections of ^{238}U in several energy groups generated by UFO are shown in Fig. 4. The results show that ^{238}U has a larger resonance capture on the fuel surface area, which is referred to as the rim effect. Many

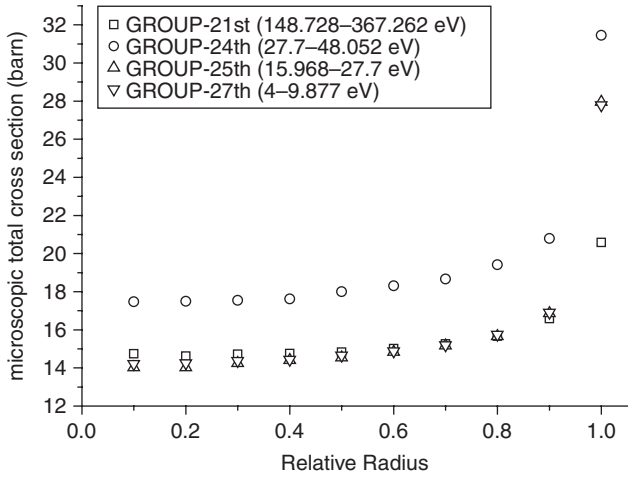

Fig. 4. Spatially dependent microscopic total cross sections of ^{238}U in the 21st, 24th, 25th, and 27th energy groups (69-group structure).

investigations have clarified that considering the spatially dependent cross sections of annular regions does not have a major impact on the resonance calculation result.[26,27] However, the two-region assumption is still inherent in the derivation of equivalence theory. Even though there have been improvements in this area, such as the spatially dependent Dancoff method and the generalized Stamm'ler method, the derivation of these methods is still based on the crucial assumption that the escape probability is calculated with a spatially constant total cross section.

There are two reasons why it is difficult to narrow down this source of deviation under the calculation scheme of equivalence theory:

1. Although the spatially dependent Dancoff method and the generalized Stamm'ler method are able to treat the distributed resonance self-shielding effect, they are based on generalization of Eq. (2). When the slowing-down equation is applied to multiple regions, with the NR approximation and a flat neutron source approximation, we have the following flux expression for region i:

$$\phi_i(E)=\sum_{j=1}^{N+1}\frac{P_{ij}(E)}{\Sigma_{tj}(E)}\Sigma_{pj}\frac{1}{E}. \tag{9}$$

An important assumption is then made, namely, that at the beginning of the calculation, the macroscopic total cross sections of all the fuel regions are the same. Equation (9) then simplifies to

$$\phi_i(E)=\frac{1}{E}\left[\frac{\Sigma_{pf}}{\Sigma_{tf}(E)}\{1-P_{im}(E)\}+P_{im}(E)\right]. \tag{10}$$

From Eq. (10), it is known that neutron collision probabilities for region i can then be calculated based on this assumption.

2. When directly compared with the results of other rigorous methods such as the ultrafine-group method, the results for the cross section show a significant part of the error caused by the NR approximation. This will be discussed in Sec. II.B.3.

However, we can still evaluate the deviation in the cross section caused by this approximation under the ultrafine-group slowing-down calculation scheme, which is similar to the treatment in Sec. II.B.1. Equation (1) is generalized to multiple regions in the UFO code:

$$\Sigma_{t,i}(E)\phi_i(E)V_i=\sum_j V_jP_{j\to i}(E)\int_0^\infty \Sigma_{s,j}(E'\to E)\phi_j(E')\,dE'. \tag{11}$$

In UFO, the probabilities are also calculated based on a flat source distribution approximation. Equation (11) is used in method 5 to consider the distributed self-shielding

effect. Both methods 3 and 5 use the ultrafine-group slowing-down calculation and the exact value of the neutron collision probability. The only difference is that method 3 ignores the distributed self-shielding effect, just like the treatment in methods 1 and 2.

The relative difference in microscopic absorption cross sections of ^{238}U calculated by methods 3 and 5 is shown in Fig. 5. In method 5, the final results for the microscopic cross section of the fuel are condensed to one region by flux weight. The maximum relative difference is $\sim 2\%$ at the 24th energy group using the results of method 5 as reference. From the result, we can see that the two-region fuel-moderator heterogeneous approximation causes overestimation of the cross section of the resonance isotope. Because the fuel has larger resonance capture on the surface area, it is harder for a neutron generated in the inner region to undergo the first collision in the moderator, which means that the exact background cross section for the inner region is smaller.

Also, the flat source distribution used in methods 3 and 5 may also cause error in the final result for the effective cross section. However, in the derivation of both equivalence theory and the ultrafine-group method, the flat source distribution approximation is essential to calculate the neutron collision probability. Thus, the difference between methods 3 and 5 does not include the error caused by this approximation.

II.B.3. Narrow Resonance Approximation

The NR approach is suitable for fast reactor core calculations because a fast reactor system is sensitive to the high-energy range where the resonances are narrow and tight. For reactor systems sensitive to energies from 1 to 500 eV, the accuracy of the NR approximation diminishes because of the resonance peaks of broad and intermediate width inside this energy range. In regular

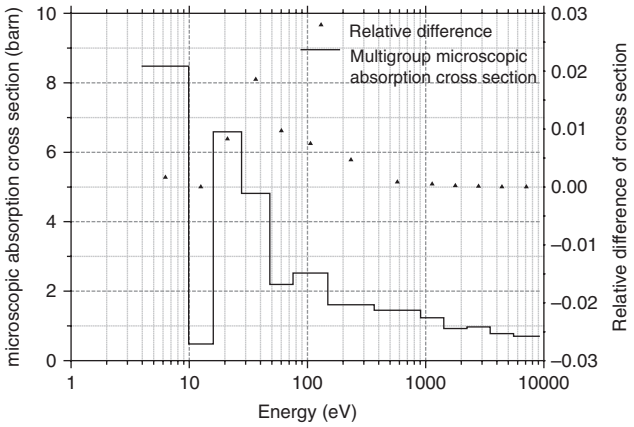

Fig. 5. Relative difference in effective microscopic cross sections (absorption) of ^{238}U calculated by methods 3 and 5, depicted with the reference absorption cross section of ^{238}U (69-group structure).

cross-section libraries, the preparation of the resonance integral table involves both the NR approximation and ultrafine-group slowing-down calculation. In this case, to have a clean evaluation of the discrepancy analysis, the ultrafine-group flux calculator UFO is used with the same nuclear data and ultrafine-group structure to perform the slowing-down calculation for heterogeneous systems and resonance integral tables.

In the derivation of Eq. (6), the resonance integral $I_{g,x}(\sigma_{0,n})$ is integrated using the NR approximated flux expression Eq. (4). However, in the practical procedure of equivalence theory, the resonance integral in the library is calculated by

$$I_{g,x}(\sigma_{0,n}) = \frac{(\sigma_{p,r}+\sigma_{0,n})\sigma_x(\sigma_{0,n})}{\sigma_{p,r}+\sigma_{0,n}+\sigma_a(\sigma_{0,n})} = \phi_{\mathrm{NR}}\cdot\sigma_x(\sigma_{0,n}), \quad (12)$$

where ϕ_{NR} is the flux expression in the numerator of Eq. (6). In the NJOY code system, for the higher-energy region where the resonances are narrow and tight, $\sigma_x(\sigma_{0,n})$ is calculated using the NR approximation, and for the epithermal region, it is calculated by direct numerical solution of the neutron slowing-down equation. In this case, $\sigma_x(\sigma_{0,n})$ for all resonance energy groups are obtained by ultrafine-group slowing-down calculation with UFO.

Based on Eqs. (5) and (12), the expression for the effective cross section from equivalence theory can be rewritten as

$$\sigma^f_{x,g} = \frac{\sum_{n=1}^{N} b_n \sigma_{x,g}(\sigma_b^n)\phi_{g,\mathrm{NR}}(\sigma_b^n)}{\sum_{n=1}^{N} b_n \phi_{g,\mathrm{NR}}(\sigma_b^n)}, \quad (13)$$

where

$$\phi_{g,\mathrm{NR}}(\sigma_b^n) = \frac{\sigma_{p,r}+\sigma_b^n}{\sigma_{p,r}+\sigma_b^n+\sigma_a(\sigma_b^n)}. \quad (14)$$

Here, $\sigma_a(\sigma_b^n)$ is the microscopic cross section of the homogeneous system that has the background cross section of σ_b^n, and $\phi_{g,\mathrm{NR}}(\sigma_b^n)$ is the scalar flux of this homogeneous system calculated by Eq. (14).

In the equivalence theory, there are two different meanings of the "NR approximation" involved. The first is that when the effective cross sections for homogeneous cases are generated, NR approximation as a specific flux shape is used. In this study, we call this NR approximation NR-homo. The second is that in the derivation of equivalence theory with multiterm rational approximation of probabilities, the effective cross sections for homogeneous cases are assumed to be calculated using the NR approximation only to make sure that the flux shape of the heterogeneous case can be expressed by Eq. (4); that is to say, the coefficients in Eq. (3) can be used to weight the

fluxes and reaction rates of multiple homogeneous cases. In this study, we call this NR approximation NR-heter. However, the effective cross sections for homogeneous cases are not necessarily calculated using NR approximation as a flux shape. In this section, we are trying to evaluate the discrepancy caused by the NR-heter approximation.

In contrast to what was done in Sec. II.B.1, method 1 is performed in the conventional procedure, not using reaction rate preservation. Then, the only difference between methods 1 and 4 is the slowing-down source evaluation in Eq. (1). The neutron collision probability in both methods 1 and 4 is calculated using Carlvik's approximation, and the distributed resonance effect is ignored in both methods. The relative differences in microscopic absorption cross sections of ^{238}U generated by the two methods in the WIMS 69-group and XMAS 172-group structures are shown in Figs. 6 and 7.

It is found that in some energy groups that have broad resonances, the maximum difference is $\sim$3%, and the effective cross section calculated by equivalence theory is overestimated. Increasing the group number of the energy group structure does not reduce this deviation. A detailed analysis of the overestimation of cross sections by the NR approximation will be given in Sec. III.A.

II.C. Multiplication Factor Calculation

Calculation of multiplication factors for a simple pin cell problem was performed to show how these approximations affect the final results of transport calculations. The pin cell consists of a UO_2 fuel pin (5 wt% ^{235}U enrichment), zirconium cladding, and H_2O moderator regions. Figure 8 and Table I show the configuration and materials for this problem. In the pin cell case, Carlvik's two-term rational approximation used in methods 1 and 4 is modified by a Dancoff factor.

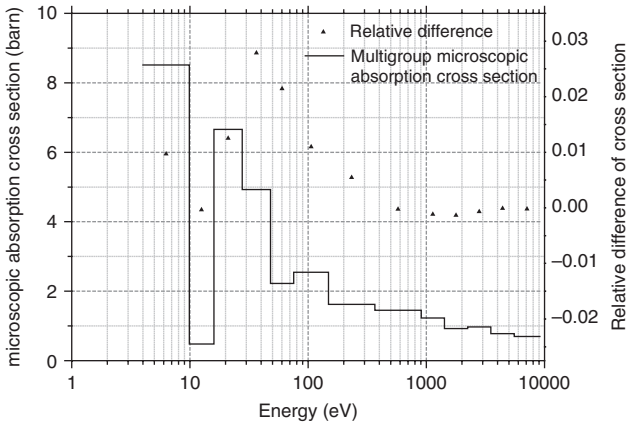

Fig. 6. Relative difference in effective microscopic cross sections (absorption) of ^{238}U calculated by methods 1 and 4, depicted with the reference absorption cross section of ^{238}U (69-group structure).

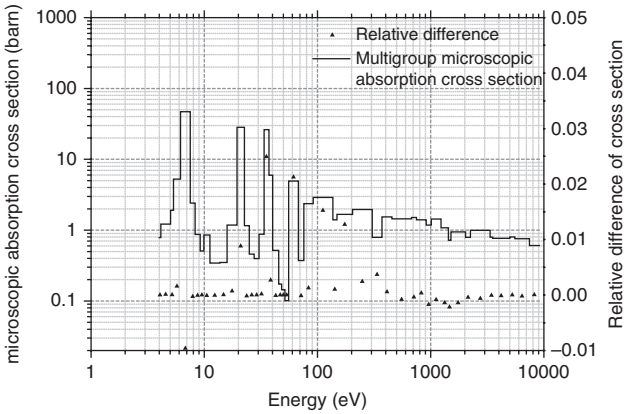

Fig. 7. Relative difference in effective microscopic cross sections (absorption) of ^{238}U calculated by methods 1 and 4, depicted with the reference absorption cross section of ^{238}U (172-group structure).

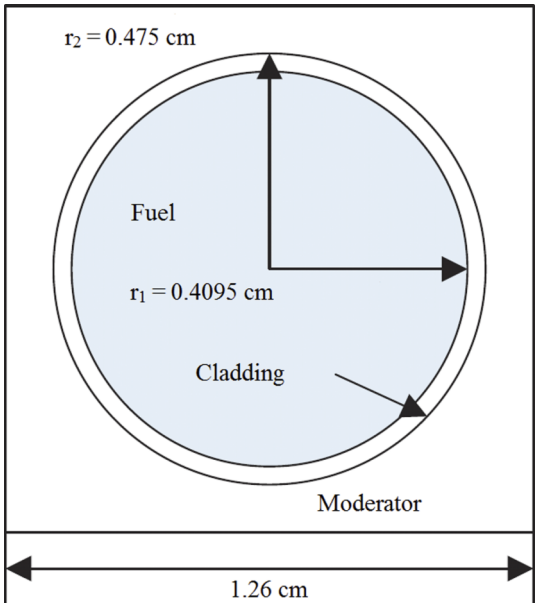

Fig. 8. Configuration of the pin cell problem.

Because all the previous analyses of resonance cross sections have been based on the assumption of just one resonance isotope, the multiplication factor calculation is performed without considering the resonance interference effect caused by ^{235}U and zirconium. The effective cross sections of ^{235}U are directly given by UFO calculation, and the effective cross sections of only ^{238}U are treated by equivalence theory. The resonance integral used in equivalence theory is generated by UFO to provide a clean evaluation. The temperatures of all the regions are assumed to be 300 K.

Table II lists the deviations of infinite multiplication factors caused by three approximations. According to the earlier discussion, we have a clean evaluation of the error

TABLE I

Material Composition of Fuel Cell

Material	Atomic Density (10^{24} atom/cm^3)				
	^{238}U	^{235}U	^{16}O	^{1}H	Zr (Natural)
Fuel	0.02194	0.001155	0.04619	—	—
Cladding	—		—	—	0.04360
Water	—		0.03362	0.06723	—

caused by rational approximation of the neutron collision probability, the two-region fuel-moderator heterogeneous system approximation, and the NR approximation without other factors that may cause error. For each case, the more rigorous method is used as reference result.

The error listed in Table II is caused by overestimation of microscopic absorption cross sections of ^{238}U only. If the resonance interference treatment adopts the conventional iteration procedure,[7] the error will be larger because the iteration procedure has a positive correction on cross sections of ^{238}U. Since the pin cell problem is more sensitive to the cross section of ^{238}U than to that of ^{235}U, the overestimation of microscopic absorption cross sections of ^{238}U is the main reason why the infinite multiplication factors become smaller.

Figures 2, 3, 5, and 6 and Table II also show that among the three approximations, the NR approximation causes the largest error in the cross section and the infinite multiplication factors. Since the pin cell problem is more sensitive to the lower-energy range, which contains broad resonances, the NR approximation is a crucial factor affecting the accuracy of resonance calculation by equivalence theory.

III. AN IMPROVED DERIVATION OF THE EFFECTIVE CROSS SECTION BY EQUIVALENCE THEORY

III.A. The Root Reason for Overestimation Caused by the NR Approximation

The effective cross section in heterogeneous system is defined as

$$\sigma_{x,g} = \frac{\int_{\Delta E_g} \sigma_x(E)\phi_{f,\mathrm{SD,heter}}(E)\,dE}{\int_{\Delta E_g} \phi_{\mathrm{SD,heter}}(E)\,dE}\ , \qquad (15)$$

where $\phi_{f,\mathrm{SD,heter}}(E)$ is the fine flux directly solved using the ultrafine-group method. The essence of equivalence theory is to evaluate the flux shape of a heterogeneous system using flux shapes of multiple homogeneous systems. The flux shape of a homogeneous system is evaluated by

$$\phi_{\mathrm{homo}}(E) = \frac{\sigma_{p,r} + \sigma_b^n}{\sigma_{p,r} + \sigma_b^n + \sigma_a(E)} \frac{1}{E}\ . \qquad (16)$$

Equation (16) is the continuous-energy form of Eq. (14).

It is well known that in the epithermal energy region, the flux depression of a broad resonance will be different from the asymptotic flux from the NR approximation. Figure 9 shows a comparison of fine-structure neutron spectra of the fuel for the case given in Sec. II.B in the energy range 27.7 to 48.052 eV, where "NR" indicates the spectrum obtained by Eq. (4) and "SD" the spectrum obtained by slowing-down calculation using the same rational approximation of probabilities, that is to say, method 4. The neutron flux is normalized such that the integral of the continuous-energy flux in this energy range is 1. It is clear from Fig. 9 that the shapes of the spectra are different. A different flux shape does not necessarily lead to a different effective cross section. However, the reaction rates calculated from the normalized neutron flux can directly show the difference in effective cross section. Figure 10 presents a comparison of the continuous-energy reaction rates obtained using the same two approaches as in Fig. 9.

TABLE II

Error in Infinite Multiplication Factors Caused by Each Approximation for the Pin Cell Problem

Approximation	Comparison of Methods	Reference Method	Error (pcm)
Rational approximation of neutron collision probability	1 and 2	2	−34.7
	3 and 4	3	−34.6
Two-region fuel-moderator heterogeneous system	3 and 5	5	−118.3
NR approximation	1 and 4	4	−222.3

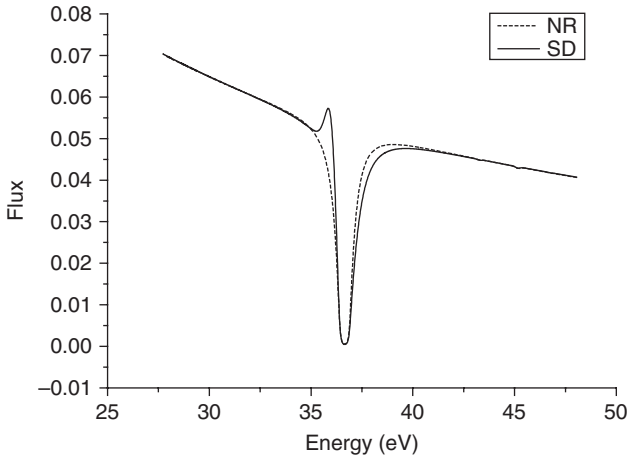

Fig. 9. Fine-structure neutron spectrum of NR and SD for the 24th group (69-group structure).

As previously stated, there are two meanings of "NR approximation" in the derivation of equivalence theory. The discrepancy shown in Sec. II.B.3 is caused by the NR-heter approximation, using the coefficients in Eq. (3) to weight the fluxes and reaction rates of multiple homogeneous cases. In our test, the effective cross section of the homogeneous case is obtained by the slowing-down calculation of UFO, so the difference shown in Fig. 10 is not equivalent to that given in Sec. II.B.3. Figure 10 shows only the difference in cross section condensed by the flux shape in Eq. (4) and the actual flux shape obtained by method 4.

Knowing that using the cross section calculated using the flux shape of the NR approximation is not appropriate, in the earlier development of equivalence theory, researchers tended to use the slowing-down calculated cross section for the homogeneous case instead of the cross section calculated by Eq. (4) as a correction. Equation (13) can be rewritten as

$$\sigma^f_{x,g} = \frac{\sum_{n=1}^{N} b_n \phi_{g,\mathrm{NR}}(\sigma_b^n) \dfrac{\int_{\Delta E_g} \sigma_x(E)\phi_{n,\mathrm{SD,homo}}(E)\,dE}{\int_{\Delta E_g} \phi_{n,\mathrm{SD,homo}}(E)\,dE}}{\sum_{n=1}^{N} b_n \phi_{g,\mathrm{NR}}(\sigma_b^n)}\,, \tag{17}$$

where $\phi_{n,\mathrm{SD,homo}}(E)$ is the spectrum of the homogeneous case in continuous-energy form calculated by the ultrafine slowing-down calculation. If the integral of this fine flux is normalized to 1, we have

$$\begin{aligned}\sigma^f_{x,g} &= \int_{\Delta E_g} \sum_{n=1}^{N} \frac{b_n \phi_{g,\mathrm{NR}}(\sigma_b^n)}{\sum_{n=1}^{N} b_n \phi_{g,\mathrm{NR}}(\sigma_b^n)} \phi_{n,\mathrm{SD,homo}}(E)\cdot\sigma_x(E)\,dE \\ &= \int_{\Delta E_g} \phi_{eq}(E)\cdot\sigma_x(E)\,dE\,. \end{aligned} \tag{18}$$

Equation (18) is the expression for the effective cross section in the practical procedure of equivalence theory, which uses multiterm rational approximations and the effective cross sections of homogeneous cases calculated by the ultrafine-group method. From Eq. (15), we have

$$\sigma^f_{x,g} = \int_{\Delta E_g} \phi_{f,\mathrm{heter}}(E)\sigma_x(E)\,dE\,. \tag{19}$$

$\phi_{f,\mathrm{heter}}(E)$ is also normalized such that its integral is 1.

Figure 11 presents a comparison of the fine-structure neutron spectra of $\phi_{eq}(E)$ and $\phi_{f,\mathrm{heter}}(E)$. Figure 12 presents a comparison of continuous-energy reaction rates calculated from $\phi_{eq}(E)$ and $\phi_{f,\mathrm{heter}}(E)$. In these figures, "EQ" means the practical procedure of equivalence theory and "SD" direct solution of the ultrafine-group slowing-down equation with the same rational approximation of probabilities. The energy range is 27.7 to 48.052 eV. Unlike Fig. 10, the difference given in Fig. 12 is equivalent to the difference given in Sec. II.B.3. Figure 13 shows the absolute difference of the two continuous-energy reaction rates. It is clear from Fig. 13 that the practical procedure of equivalence theory causes overestimation of the effective cross section. A large number of cases using different rational approximations in different energy groups have been tested, and the discrepancy in cross sections always exists in different levels.

According to Sec. II.A, the derivation of equivalence theory is based on the assumption that the flux shape of the homogeneous case can be expressed as Eq. (4). However, in the practical procedure of equivalence theory, the flux shape of the homogeneous case is solved using the ultrafine-group method, while the weight of each homogeneous case is still based on the NR approximation.

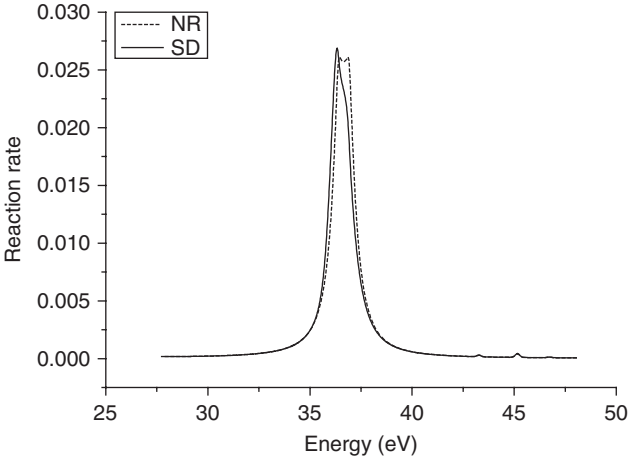

Fig. 10. Continuous-energy reaction rates of NR and SD for the 24th group (69-group structure).

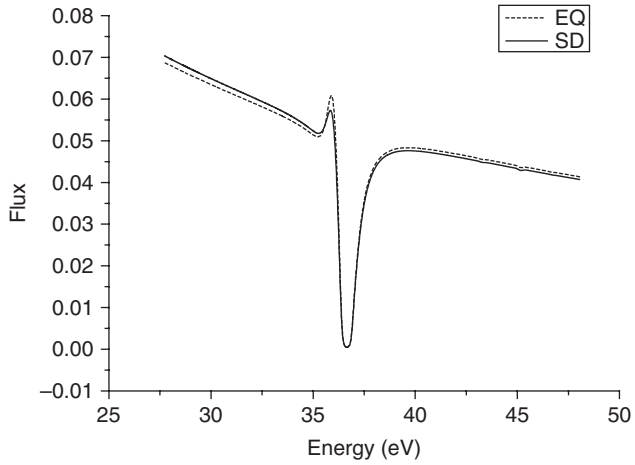

Fig. 11. Fine-structure neutron spectrum of EQ and SD for the 24th group (69-group structure).

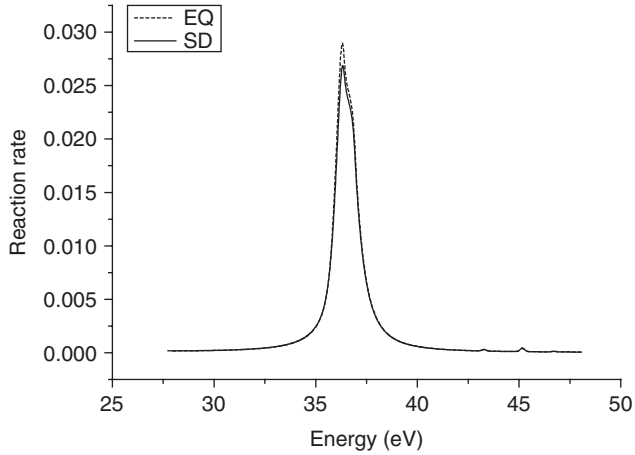

Fig. 12. Continuous-energy reaction rates of EQ and SD for the 24th group (69-group structure).

This procedure itself is a contradiction. The original intention of this treatment seems to be a correction of the cross sections of homogeneous cases to fix the final results of the heterogeneous problem. However, this correction is actually proposed in an intuitive manner without rigorous theoretical derivation. The results in Fig. 13 show that the error of this treatment still exists in different levels and is usually an overestimation.

III.B. The Improved Method Based on the Flux Shape of Solving the Slowing-Down Equation

As previously discussed, using the effective cross section calculated by the ultrafine-group method in Eq. (13) is actually an empirical correction to the NR-homo approximation mentioned in Sec. II.B.3.

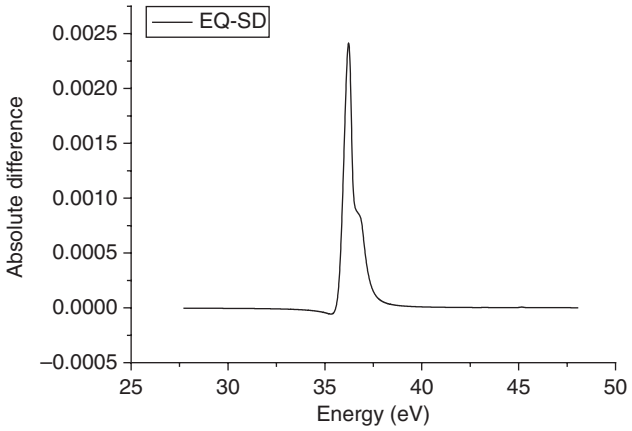

Fig. 13. Absolute difference of continuous-energy reaction rates for the 24th group (69-group structure).

Since the essence of equivalence theory is to evaluate the flux shape of heterogeneous system by multiple homogeneous cases, for an energy group containing a large resonance, correction based on the NR-heter approximation may work better. With the use of the reciprocity theorem, Eq. (1) is rewritten as

$$\Sigma_{t,f}(E)\phi_f(E) = \left(1 - P_{fm}(E)\right) \int_0^\infty \Sigma_{s,f}(E' \to E)\phi_f(E')\, dE' + \frac{P_{fm}(E)\Sigma_{t,f}(E)}{\Sigma_{t,m}(E)} \int_0^\infty \Sigma_{s,m}(E' \to E)\phi_m(E')\, dE' . \quad (20)$$

If the collision probability from fuel to moderator is approximated as Eq. (3),

$$P_{fm}(E) = \sum_{n=1}^{N} \frac{b_n a_n}{\Sigma_{t,f}(E)\bar{l} + a_n} = \sum_{n=1}^{N} b_n P_n(E) \ , \quad (21)$$

then Eq. (20) is rewritten as

$$\Sigma_{t,f}(E)\phi_f(E) = \sum_{n=1}^{N} b_n (1 - P_n(E)) \int_0^\infty \Sigma_{s,f}(E' \to E)\phi_f(E')\, dE' + \sum_{n=1}^{N} b_n \frac{P_n(E)\Sigma_{t,f}(E)}{\Sigma_{t,m}(E)} \times \int_0^\infty \Sigma_{s,m}(E' \to E)\phi_m(E')\, dE' . \quad (22)$$

Suppose that there is a two-region problem having a fuel rod with a specific geometry and that the fuel-moderator collision probability is exactly $P_n(E)$:

$$P_n(E)=\frac{a_n}{\Sigma_{t,f}(E)\bar{l}+a_n}\ . \tag{23}$$

We then have

$$\Sigma_{t,f}(E)\phi_{fn}(E)=(1-P_n(E))\int_0^\infty \Sigma_{s,f}(E'\to E)\phi_{fn}(E')\,dE' + \frac{P_n(E)\Sigma_{t,f}(E)}{\Sigma_{t,m}(E)}\int_0^\infty \Sigma_{s,m}(E'\to E)\phi_{mn}(E')\,dE'. \tag{24}$$

From Eqs. (22) and (24), we propose an approximate expression for $\phi_f(E)$:

$$\phi_f(E)\approx\sum_{n=1}^{N} b_n\phi_{fn}(E)\,. \tag{25}$$

Equation (25) is then rewritten as

$$\sigma_{x,g}=\frac{\sum_{n=1}^{N} b_n\int_{\Delta E_g}\sigma_x(E)\phi_{fn}(E)\,dE}{\sum_{n=1}^{N} b_n\int_{\Delta E_g}\phi_{fn}(E)\,dE} =\frac{\sum_{n=1}^{N} b_n\int_{\Delta E_g}\phi_{fn}(E)\,dE\cdot\frac{\int_{\Delta E_g}\sigma_x(E)\phi_{fn}(E)\,dE}{\int_{\Delta E_g}\phi_{fn}(E)\,dE}}{\sum_{n=1}^{N} b_n\int_{\Delta E_g}\phi_{fn}(E)\,dE} =\frac{\sum_{n=1}^{N} b_n\phi_{n,\mathrm{SD,heter}}(\sigma_b^n)\cdot\sigma_{x,n}(\sigma_b^n)}{\sum_{n=1}^{N} b_n\phi_{n,\mathrm{SD,heter}}(\sigma_b^n)}\ , \tag{26}$$

where

$$\sigma_{b,n}=\sigma_{0,f}+\sigma_{p,r}+a_n/N_r\bar{l}\ ,$$

$$\sigma_{x,n}(\sigma_b^n)=\frac{\int_{\Delta E_g}\sigma_x(E)\phi_{fn}(E)\,dE}{\int_{\Delta E_g}\phi_{fn}(E)\,dE}\ ,$$

and

$$\phi_{n,\mathrm{SD,heter}}(\sigma_b^n)=\int_{\Delta E_g}\phi_{fn}(E)\,dE\,.$$

Here, $\phi_{n,\mathrm{SD,heter}}(\sigma_b^n)$ is still the integrated flux solved by the ultrafine-group method in the heterogeneous case, and it is time-consuming to solve the flux shape each time. Fortunately, for the heterogeneous case solved by Eq. (24),

$$\sigma_{x,n}(\sigma_b^n)=\frac{\int_{\Delta E_g}\sigma_x(E)\phi_{fn}(E)\,dE}{\int_{\Delta E_g}\phi_{fn}(E)\,dE} \approx\frac{\int_{\Delta E_g}\sigma_x(E)\phi_{fn,\mathrm{homo}}(E)\,dE}{\int_{\Delta E_g}\phi_{fn,\mathrm{homo}}(E)\,dE}\ , \tag{27}$$

where $\phi_{fn,\mathrm{homo}}(E)$ is the continuous-energy flux in the homogeneous case with background cross section σ_b^n solved by the ultrafine-group method. Table III shows the relative difference in the effective cross sections using $\phi_{fn,\mathrm{homo}}(E)$ and $\phi_{fn,\mathrm{heter}}(E)$. The integrated flux can be replaced with the homogeneous case without sacrificing too much accuracy. The final expression for the effective cross section is

$$\sigma_{x,g}=\frac{\sum_{n=1}^{N} b_n\phi_{n,\mathrm{SD,homo}}(\sigma_b^n)\cdot\sigma_{x,n}(\sigma_b^n)}{\sum_{n=1}^{N} b_n\phi_{n,\mathrm{SD,homo}}(\sigma_b^n)}\ ,$$

$$\phi_{n,\mathrm{SD,homo}}(\sigma_b^n)=\int_{\Delta E_g}\phi_{fn,\mathrm{homo}}(E)\,dE\,. \tag{28}$$

The conventional procedure of equivalence theory is interpolation of the resonance integral table with the background cross section given by Eq. (3) and using Eq. (5) or Eq. (13) to calculate the effective cross section. The scalar fluxes of homogeneous systems also correspond to the background cross section. There is no need to set up a $\phi_{g,\mathrm{NR}}^r$ table for interpolation, because the fluxes can always be calculated by Eq. (14) under the NR approximation.

Unlike the conventional procedure of equivalence theory, Eq. (28) involves an integrated flux solved by ultrafine-group theory. Figure 14 gives the dependence of the effective cross section (absorption) and the correspondent integrated fluxes $\phi_{n,\mathrm{SD,homo}}$ of ^{238}U on the background cross section. It shows that the dependence of the integrated fluxes on the background cross section is also a reasonably smooth function, like the dependence of the effective cross section on the background cross section. Therefore, the integrated fluxes can also be tabulated for discrete values of background cross sections and temperatures. Although Fig. 14 shows that the smooth functional behavior of the integrated fluxes is different from that of the effective cross section, based on much research into the interpolation of the resonance integral table,[24] a high-order polynomial function or a logarithmic function can always be found to increase the accuracy of the interpolation.

TABLE III

Relative Difference in Effective Cross Sections of ^{238}U Calculated Using $\phi_{fn,\text{homo}}(E)$ and $\phi_{fn,\text{heter}}(E)$ for Different Energy Groups and Background Cross Sections*

Energy Group[a]	Background Cross Section/a_n (%)[b]						
	50/1.0	70/1.4	100/2.0	150/3.0	200/4.0	300/6.0	500/10.0
15	0.02	0.02	0.01	0.01	0.01	0.00	0.00
16	0.00	0.00	0.00	0.00	0.00	0.00	0.00
17	0.02	0.02	0.01	0.01	0.01	0.01	0.01
18	0.02	0.02	0.02	0.02	0.01	0.01	0.01
19	0.05	0.04	0.04	0.03	0.03	0.02	0.02
20	0.03	0.03	0.03	0.02	0.02	0.02	0.01
21	0.24	0.21	0.18	0.16	0.13	0.12	0.09
22	0.29	0.28	0.26	0.23	0.21	0.18	0.15
23	−0.28	−0.20	−0.13	−0.07	−0.04	−0.01	0.01
24	0.09	0.12	0.14	0.16	0.18	0.18	0.19
25	0.09	0.08	0.08	0.08	0.08	0.07	0.07
26	0.06	0.05	0.03	0.02	0.02	0.01	0.01
27	−0.65	−0.60	−0.54	−0.47	−0.43	−0.38	−0.32

*The relative difference is given by $(\sigma_{x,n,\text{heter}} - \sigma_{x,n,\text{homo}})/\sigma_{x,n,\text{homo}}$.
[a]The energy group structure is WIMS 69-group.
[b]Background cross section is for homogeneous cases and a_n is for heterogeneous cases calculated using Eq. (23).

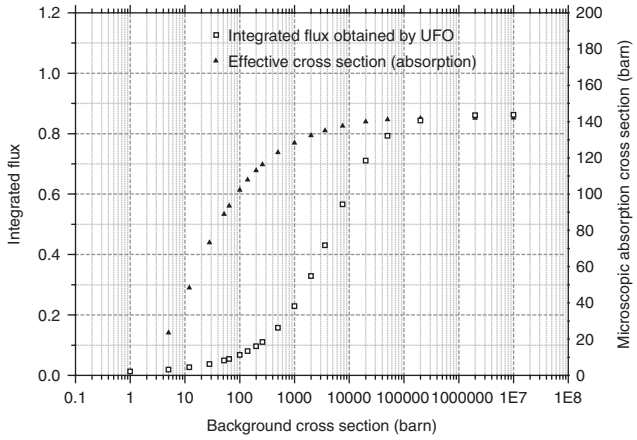

Fig. 14. Variation in effective cross section (absorption) and corresponding integrated fluxes of ^{238}U at 300 K for the 27th enhanced neutron current group (69-group structure).

The conventional calculation procedures of equivalence theory with multiterm rational approximation can be improved as follows:

1. Effective cross sections and the integrated fine-structure fluxes of homogeneous cases with different background cross sections and temperature are generated by the ultrafine-group flux calculator and tabulated in the cross-section library.

2. The coefficients of Eq. (3) are evaluated by Dancoff factor or other methods.

3. Effective cross sections and integrated fluxes for a desired background cross section and temperature are calculated by interpolation from the resonance integral tables.

4. Equation (28) is used to calculate the effective cross sections of heterogeneous systems.

The only difference between the improved procedures and the conventional ones is that the improved method involves interpolation on the integrated flux table by the background cross section. Preparation of the integrated flux table does not require any extra calculational effort, because when calculating the effective cross section, the integrated flux is already known. The extra storage needed in the library and the extra calculation involved in the interpolation have almost no effect on the computational efficiency of equivalence theory.

III.C. Numerical Results

The validity of the present method is tested by several test calculations using different geometries, different energy group structures, and different ultrafine-group slowing-down solvers. Four types of geometry are used: isolated fuel pin, isolated fuel plate, pin cell, and multicell lattice. These four cases are tested with only one resonance isotope, ^{238}U. The pin cell case given in Sec. II.C is used for calculation of the infinite multiplication factors. To distinguish the two pin cell cases, including the pin cell case mentioned in Sec. II.C, for the infinite multiplication test, we denote the pin cell with

only ^{238}U as pin-cell-single. The calculation conditions are as follows:

1. The geometry of the multicell lattice is shown in Fig. 15. Fuel rod 6 is selected as the target position to test the improved method.

2. For the isolated fuel pin, pin-cell-single, and the multicell lattice, the fuel diameter is 1.0 cm.

3. For the isolated fuel plate, the fuel thickness is 0.5 cm.

4. For pin-cell-single and the multicell lattice, the cell pitch is 1.418 cm.

5. The fuel consists of only ^{238}U with $N_{238} = 0.02 \times 10^{24}$ atoms/cm^3.

6. For the isolated fuel pin, pin-cell-single, and the multicell lattice, the rational approximation is given by Carlvik's two-term rational approximation and the Dancoff factor. The Dancoff factor is calculated by the neutron current method.[28]

7. For the isolated fuel plate, the rational approximation is given by Roman's two-term rational approximation: $b_1 = 1.1, b_2 = -0.1, a_1 = 1.4, a_2 = 5.4$ (Ref. 7).

8. The resonance integral used in equivalence theory is generated by UFO calculations on a homogeneous system of different N_H/N_{238} compositions.

9. The energy group structures are WIMS 69-group and XMAS 172-group.

10. The other ultrafine-group slowing-down solvers tested are NJOY and RMET21 (Ref. 29).

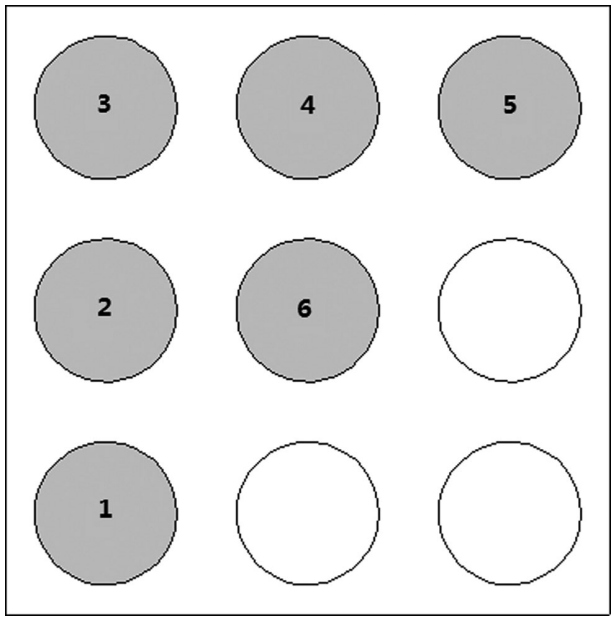

Fig. 15. Configuration of the multicell lattice problem.

11. The calculation of infinite multiplication factors is performed in the pin cell case given in Sec. II.C, which is a typical light water reactor (LWR) pin cell.

The conventional Stamm'ler method (method 1) is modified using the new procedure mentioned in Sec. III.A. Reference results are given by method 4 as specified in Sec. II.B. For each case, Carlvik's approximation used in method 1, improved method 1, and method 4 is replaced by the correspondent rational approximation. It should be noted that in this test, the effective cross section and integrated fluxes for a desired background cross section are directly calculated by UFO instead of by interpolation in the library, to avoid the error caused by interpolation.

Figures 16 through 21 show the relative errors in the microscopic absorption cross section of ^{238}U generated by method 1 and improved method 1, using the results of method 4 as reference. The new method gives improved results, with a reduction in the microscopic cross section, especially at energy groups in the epithermal energy

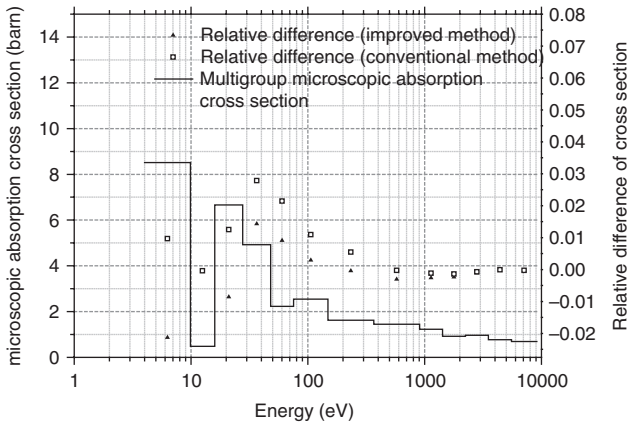

Fig. 16. Comparison of microscopic absorption cross sections of ^{238}U in isolated fuel pin (69-group structure).

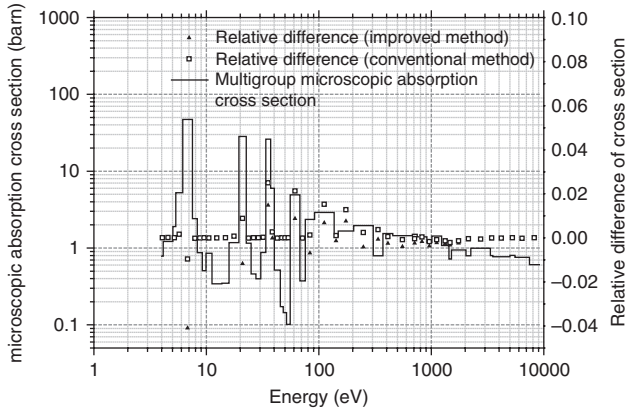

Fig. 17. Comparison of microscopic absorption cross sections of ^{238}U in isolated fuel pin (172-group structure).

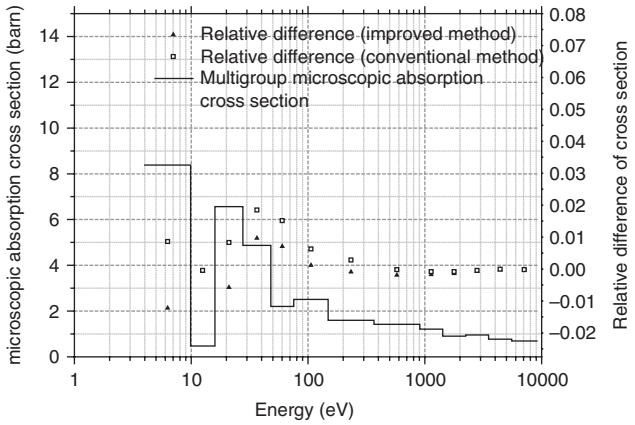

Fig. 18. Comparison of microscopic absorption cross sections of ^{238}U in isolated fuel plate (69-group structure).

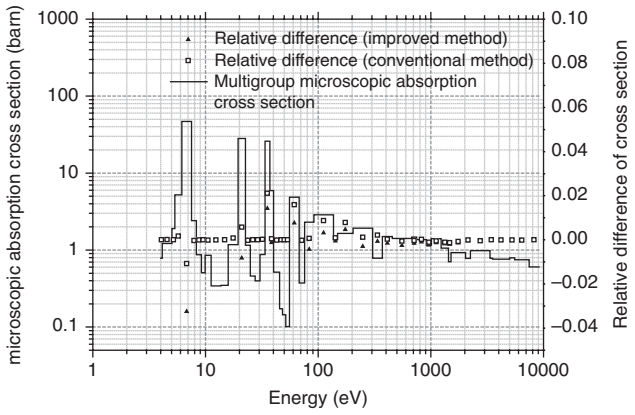

Fig. 19. Comparison of microscopic absorption cross sections of ^{238}U in isolated fuel plate (172-group structure).

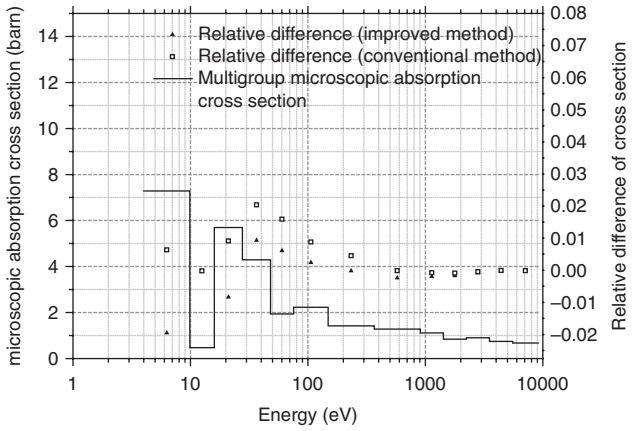

Fig. 20. Comparison of microscopic absorption cross sections of ^{238}U in pin-cell-single (69-group structure).

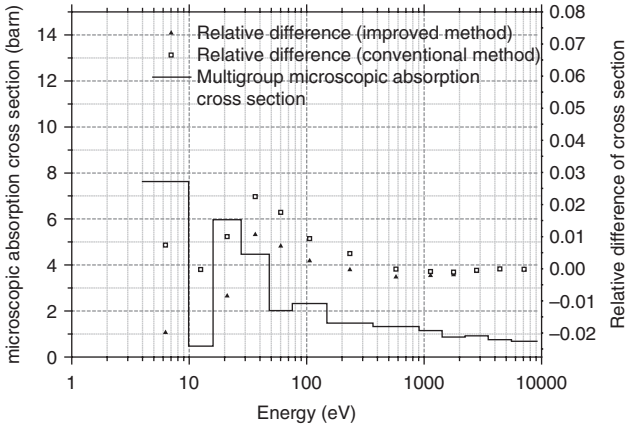

Fig. 21. Comparison of microscopic absorption cross sections of ^{238}U in multicell lattice (69-group structure).

region. Figures 16 through 19 show that this improvement works well in both cylindrical and slab geometries. The correction effect works on both the WIMS 69-group and XMAS 172-group structures. Figures 20 and 21 show that the improved method can be used in practical lattice configuration because the improved method also gives a correction effect on the cross section with different Dancoff factors involved.

The improvement is based on the assumption of Eq. (25). Like the earlier improvement using the effective cross section of the homogeneous case calculated by the ultrafine-group method instead of the NR approximation, this improvement is proposed without rigorous theoretical derivation. In Fig. 20, the difference in the cross section in some energy groups is reduced to $<1\%$, but in the 27th group, the difference in the cross section increases to -2%. The improvement in the accuracy of the effective cross section per group is not as good as with the rigorous ultrafine-group method. However, this improvement is more valuable in the calculation of the infinite multiplication factors. The large error for the 6-eV resonance of ^{238}U has a dominant effect in LWR analysis. It will cancel out the overestimation caused by other groups and the other two basic approximations. In the pin cell problem, the improved procedure corrects the multiplication factors by $\sim$200 to 300 pcm because of the reduction in the ^{238}U absorption cross sections in the epithermal energy region. Table IV compares the infinite multiplication factors of the pin cell case in Sec. II.C obtained by the five methods. The improvement in the present study focuses on the NR approximation; however, it can be seen that the correction of improved method 1 almost covers the error caused by all three basic approximations, and the accuracy of equivalence theory with multiterm rational approximation will be improved without empirical correction of the resonance integral of ^{238}U. We also present a comparison of the multigroup microscopic absorption reaction rates of ^{238}U in this case. Table V shows that the error is reduced

TABLE IV

Comparison of Infinite Multiplication Factors for Pin Cell Problem

Method	K_{inf}	Error (pcm)
Method 5 (reference)	1.485015	—
Method 3 (two-region approximation)	1.483832	−118
Method 4 (two-region approximation + rational approximation)	1.483485	−153
Method 1 (two-region approximation + rational approximation + NR approximation)	1.481262	−375
Improved method 1 (two-region approximation + rational approximation)	1.484618	−40

with the effective cross section obtained by the improved method. In addition, the improvement only works well in most of the LWR analysis, whereas the correction effect is not obvious in the fast reactor configuration.

We also test this improvement for Rowland's LWR pin cell benchmarks. Four uranium oxide (UOX) cell cases are calculated: isothermal (293 K), reduced density, fuel at 900 K, and isothermal (550 K). For mixed-oxide (MOX) fuel, four cases with different compositions and temperatures are calculated. The details of these cases are presented in Ref. 30. The calculation uses the WIMS 69-group structure and the ENDF/B-VI.8 library. The results of UFO (method 5) are selected as reference. The boundary condition is cylindrical and the cell is a zero-leakage one. The resonance interference effect caused by ^{235}U and zirconium is also ignored by using the cross section obtained by rigorous methods. The results in Tables VI and VII show that the improved method could fix the error in multiplication factors in most LWR cases.

Noticing that some existing lattice codes already use integrated fluxes recovered from the flux calculator in NJOY and that this still leads to overestimation of the resonance capture in ^{238}U, we present a comparison of results using integrated fluxes recovered from NJOY, RMET21, and UFO. The test case is the isolated fuel rod, and the ultrafine-group flux solver is replaced in both method 4 and in the calculations of integrated fluxes and effective cross sections. The rational approximation is Carlvik's two-term approximation.

Tables VIII, IX, and X show that RMET21 and UFO have similar correction effects on resonance energy groups 21 through 27 and that using integrated fluxes recovered from NJOY does not improve the results. In this case, two homogeneous cases are involved, because we use Carlvik's two-term rational approximation. In this case, the background cross sections of these two

TABLE V

Comparison of Multigroup Microscopic Absorption Reaction Rates of ^{238}U in Pin Cell Problem

Energy Group	Reaction Rate (Arbitrary Units)			Relative Difference (%)	
	Reference[a]	Original[b]	Improved	Original	Improved
15	1.8102E−01	1.8090E−01	1.8049E−01	−0.07	−0.29
16	1.7760E−01	1.7737E−01	1.7694E−01	−0.13	−0.37
17	2.1568E−01	2.1514E−01	2.1456E−01	−0.25	−0.52
18	2.0203E−01	2.0148E−01	2.0084E−01	−0.27	−0.59
19	2.6291E−01	2.6267E−01	2.6171E−01	−0.09	−0.46
20	5.9973E−01	6.0006E−01	5.9707E−01	0.05	−0.44
21	6.4595E−01	6.5681E−01	6.5167E−01	1.68	0.89
22	7.2537E−01	7.4230E−01	7.3513E−01	2.33	1.34
23	4.1996E−01	4.3541E−01	4.2952E−01	3.68	2.28
24	1.0211E+00	1.0705E+00	1.0556E+00	4.84	3.39
25	1.2818E+00	1.3092E+00	1.2830E+00	2.14	0.10
26	8.8053E−02	8.8009E−02	8.7891E−02	−0.05	−0.18
27	2.3709E+00	2.3986E+00	2.3332E+00	1.17	−1.59
Sum	8.1920E+00	8.3384E+00	8.2077E+00	1.79	0.19
Maximum				4.84	3.39
Average				1.16	0.27
Root-mean-square				1.97	1.28

[a]The reference results are obtained by method 4.
[b]The original method means method 1.

TABLE VI

UOX Pin Cell Results

	Case 1 (Isothermal, 293 K)	Case 2 (Reduced H_2O Density)	Case 3 (Fuel at 900 K)	Case 4 (Isothermal, 550 K)
UFO	1.38402	1.33043	1.29641	1.31108
Method 1	1.38198	1.32842	1.29440	1.30894
ΔK_{inf} (pcm)	−204	−201	−201	−214
Improved method 1	1.38418	1.33077	1.29715	1.31165
ΔK_{inf} (pcm)	16	34	74	57

TABLE VII

MOX Pin Cell Results

	Fuel 1 (Isothermal, 300 K)	Fuel 1 (Isothermal, 560 K)	Fuel 2 (Isothermal, 300 K)	Fuel 2 (Isothermal, 560 K)
UFO	1.21453	1.20038	1.26765	1.25387
Method 1	1.21315	1.19924	1.26515	1.25149
ΔK_{inf} (pcm)	−137	−114	−251	−237
Improved Method 1	1.21458	1.20092	1.26666	1.25331
ΔK_{inf} (pcm)	5	53	−99	−55

TABLE VIII

Comparison of Original and Improved Methods Using NJOY as Flux Solver

	Effective Cross Section (barn)			Relative Difference (%)		
Energy Group	Reference[a]	Original[b]	Improved	Original	Improved	Ratio ϕ_{100}/ϕ_{150}
15	0.6973	0.6932	0.6930	−0.58	−0.61	0.9918
16	0.7761	0.7652	0.7648	−1.40	−1.45	0.9906
17	0.9687	0.9596	0.9585	−0.94	−1.05	0.9889
18	0.9235	0.9109	0.9101	−1.36	−1.45	0.9931
19	1.2307	1.2275	1.2275	−0.26	−0.26	0.9966
20	1.4512	1.4393	1.4392	−0.82	−0.82	0.9959
21	1.6224	1.6306	1.6305	0.50	0.50	0.9959
22	2.5481	2.5760	2.5756	1.10	1.08	0.9934
23	2.2251	2.2692	2.2688	1.98	1.96	0.9945
24	4.9258	5.0766	5.0756	3.06	3.04	0.9880
25	6.6608	6.7739	6.7710	1.70	1.65	0.9851
26	0.4789	0.4789	0.4789	−0.01	−0.01	0.9983
27	8.5116	8.5172	8.5123	0.07	0.01	0.9818

[a]The reference results are obtained by method 4.
[b]The original method means method 1.

homogeneous cases are 100 and 150 barns. We can focus on the ratio between the integrated fluxes of these cases. This ratio directly decides the final result for the effective cross section because the integrated fluxes are used as weights. In this case, not only the shape of the flux but also the scalar flux of each homogeneous case affect the correction effect. The ratios for RMET21 and UFO are similar because both solve the slowing-down equation from an energy point near 10 keV. The ratios for NJOY and the NR approximation are similar because NJOY solves the slowing-down equation usually from an energy point near 1.8 keV, and above this energy point,

TABLE IX

Comparison of Original and Improved Methods Using UFO as Flux Solver

Energy Group	Effective Cross Section (barn)			Relative Difference (%)		Ratio ϕ_{100}/ϕ_{150}
	Reference[a]	Original[b]	Improved	Original	Improved	
15	0.6973	0.6971	0.6971	−0.02	−0.03	0.9972
16	0.7761	0.7760	0.7759	−0.01	−0.02	0.9956
17	0.9687	0.9681	0.9676	−0.07	−0.11	0.9936
18	0.9235	0.9222	0.9213	−0.14	−0.23	0.9927
19	1.2307	1.2293	1.2275	−0.12	−0.26	0.9904
20	1.4512	1.4508	1.4467	−0.02	−0.31	0.9870
21	1.6224	1.6313	1.6218	0.55	−0.04	0.9832
22	2.5481	2.5760	2.5556	1.10	0.30	0.9767
23	2.2251	2.2728	2.2454	2.14	0.91	0.9738
24	4.9258	5.0632	4.9964	2.79	1.43	0.9634
25	6.6608	6.7441	6.6040	1.25	−0.85	0.9542
26	0.4789	0.4787	0.4786	−0.04	−0.06	0.9626
27	8.5116	8.5941	8.3306	0.97	−2.13	0.9386

[a]The reference results are obtained by method 4.
[b]The original method means method 1.

TABLE X

Comparison of Original and Improved Methods Using RMET21 as Flux Solver

Energy Group	Effective Cross Section (barn)			Relative Difference (%)		Ratio ϕ_{100}/ϕ_{150}
	Reference[a]	Original[b]	Improved	Original	Improved	
15	0.6973	0.6918	0.6918	−0.79	−0.79	0.9970
16	0.7761	0.7701	0.7700	−0.77	−0.78	0.9957
17	0.9687	0.9626	0.9622	−0.63	−0.67	0.9938
18	0.9235	0.9164	0.9156	−0.76	−0.85	0.9931
19	1.2307	1.2208	1.2193	−0.80	−0.93	0.9913
20	1.4512	1.4437	1.4401	−0.52	−0.76	0.9881
21	1.6224	1.6280	1.6196	0.34	−0.17	0.9846
22	2.5481	2.5682	2.5488	0.79	0.03	0.9775
23	2.2251	2.2741	2.2475	2.20	1.01	0.9743
24	4.9258	5.0707	5.0048	2.94	1.60	0.9636
25	6.6608	6.7700	6.6274	1.64	−0.50	0.9536
26	0.4789	0.4794	0.4793	0.11	0.09	0.9610
27	8.5116	8.5749	8.2955	0.74	−2.54	0.9360

[a]The reference results are obtained by method 4.
[b]The original method means method 1.

the flux is calculated using the NR approximation. Thus, the improved method requires an ultrafine-group slowing-down solver that can solve the slowing-down equation from an energy point near 10 keV.

In addition to the topics of the present study, the improvement has several other advantages:

1. When calculating the effective cross sections of homogeneous systems, the integrated fine-structure fluxes are necessary. In other words, no additional calculations are involved in the construction of the resonance flux and resonance cross-section tables in the library.

2. The new method using the same coefficients in the multiterm rational approximation of conventional equivalence theory can be applied to irregular geometries.

3. The improvement is very simple and can be easily adopted in the lattice physics code utilizing equivalence theory.

IV. CONCLUSIONS

We presented a detailed analysis of the deviation of the resonance cross section caused by three basic approximations adopted in equivalence theory. The results show that the NR approximation is the main source of error. A detailed analysis of the NR approximation explains the root reason why it causes overestimation of the resonance capture of ^{238}U. There is an implicit correction in the practical procedure of equivalence theory, which uses the effective cross section of a homogeneous system obtained by the ultrafine-group method. This correction is not effective enough to fix the discrepancy. This conclusion leads to an attempt to correct the weighting flux. Based on the assumption that the slowing-down solved flux shape can also be separated, a new derivation of the effective cross section using the slowing-down solved integrated flux is proposed to improve the conventional method and the calculation flow. The results show that the deviation caused by conventional equivalence theory is corrected systematically by the new method. Because the new method is simple and efficient, it can be conveniently implemented into the existing codes based on equivalence theory.

ACKNOWLEDGMENTS

This work is supported by the National Natural Science Foundation of China grant 91126005 and the National High Technology Research and Development Program (863 Program) of China grant 2013AA051402.

REFERENCES

1. Y. ISHIGURO, "PEACO-II: A Code for Calculation of Effective Cross Sections in Heterogeneous Systems," JAERI-M 5527, Japan Atomic Energy Research Institute (1974).

2. M. N. NIKOLEAV et al., "The Method of Subgroups for Considering the Resonance Structure of Cross Sections in Neutron Calculations," *Sov. At. Energy*, **5**, 528 (1971); http://dx.doi.org/10.1007/BF01408755.

3. A. M. WEINBERG and E. P. WIGNER, *The Physical Theory of Neutron Chain Reactors*, University of Chicago Press, Chicago, Illinois (1958).

4. I. I. BONDARENKO, *Group Constants for Nuclear Reactor Calculations*, Consultants Bureau, New York (1964).

5. M. J. ROTH, "The WIMS-E Module W-HEAD," AEEW-R 1322, United Kingdom Atomic Energy Authority (1980).

6. R. E. MacFARLANE and D. W. MUIR, "The NJOY Nuclear Data Processing System Version 91," LA-12740-M, Los Alamos National Laboratory (1994).

7. R. J. J. STAMM'LER and M. J. ABBATE, *Methods of Steady-State Reactor Physics in Nuclear Design*, Academic Press, London (1983).

8. S. G. HONG and K. S. KIM, "Iterative Resonance Self-Shielding Methods Using Resonance Integral Table in Heterogeneous Transport Lattice Calculations," *Ann. Nucl. Energy*, **38**, 32 (2011); http://dx.doi.org/10.1016/j.anucene.2010.08.022.

9. M. EDUNIUS et al., "CASMO-3 A Fuel Assembly Burnup Program Methodology," STUDSVIK/NFA-89/2, Studsvik (1991).

10. J. R. ASKEW, "A General Description of the Lattice Code WIMS," *J. Br. Nucl. Energy Soc.*, **5**, 564 (1966).

11. H. MATSUMOTO, M. OUISLOUMEN, and T. TAKEDA, "Development of Spatially Dependent Resonance Shielding Method," *J. Nucl. Sci. Technol.*, **42**, 688 (2005); http://dx.doi.org/10.1080/18811248.2004.9726438.

12. A. HEBERT and G. MARLEAU, "Generalization of the Stamm'ler Method for the Self-Shielding of Resonant Isotopes in Arbitrary Geometries," *Nucl. Sci. Eng.*, **108**, 230 (1991); http://dx.doi.org/10.13182/NSE90-57.

13. A. YAMAMOTO, "Evaluation of Background Cross-Section for Heterogeneous and Complicated Geometry by the Enhanced Neutron Current Method," *J. Nucl. Sci. Technol.*, **45**, 1287 (2008); http://dx.doi.org/10.1080/18811248.2008.9711916.

14. H. HURIA and M. OUISLOUMEN, "ENDF/B-VI: ^{238}U Resonance Integral Reduction—A Closer Look," *Trans. Am. Nucl. Soc.*, **76**, 329 (1997).

15. M. EDINIUS, "Adjustment of the Effective ^{238}U Resonance Integral to Force Agreement with Integral Data," *Proc. Seminar ^{238}U Resonance Capture*, New York, March 18–20, 1975.

16. J. R. ASKEW, "A Characteristics Formulation of the Neutron Transport Equation in Complicated Geometries," AEEWM1108, United Kingdom Atomic Energy Authority (1972).

17. M. L. WILLIAMS and K. S. KIM, "The Embedded Self-Shielding Method," *Proc. Int. Conf. Physics of Reactors (PHYSOR 2012)*, Knoxville, Tennessee, April 15–20, 2012, American Nuclear Society (2012).

18. N. SUGIMURA and A. YAMAMOTO, "Resonance Treatment Based on Ultra-Fine-Group Spectrum Calculation in the AEGIS Code," *J. Nucl. Sci. Technol.*, **44**, 958 (2007); http://dx.doi.org/10.1080/18811248.2007.9711335.

19. Y. QIN et al., "Resonance Calculation Code UFOP Based on the Hyper-Fine Group Neutron Resonance Calculation Method," *Proc. 18th Int. Conf. Nuclear Engineering*, Xi'an, China, May 17–21, 2010.

20. M. J. HALSALL, "A Review of the WIMS Nuclear Data Library," *Nucl. Energy*, **30**, 285 (1991).

21. E. SARTORI, "Standard Energy Group Structures of Cross Section Libraries for Reactor Shielding, Reactor Cell and Fusion Neutronics Applications: VITAMIN-J, ECCO-33, ECCO-2000 and XMAS," JEF/DOC-315, Rev. 3, NEA Data Bank, Nuclear Energy Agency (1990).

22. B. R. SEHGAL and R. GOLDSTEIN, "Intermediate Resonance Absorption in Heterogeneous Media," *Nucl. Sci. Eng.*, **25**, 174 (1966); http://dx.doi.org/10.13182/NSE66-2.

23. M. L. WILLIAMS, "Correction of Multigroup Cross Sections for Resolved Resonance Interference in Mixed Absorbers," *Nucl. Sci. Eng.*, **83**, 37 (1983); http://dx.doi.org/10.13182/NSE83-2.

24. M. SEGEV, "Interpolation of Resonance Integrals," *Nucl. Sci. Eng.*, **17**, 113 (1981); http://dx.doi.org/10.13182/NSE81-2.

25. Q. ZHANG et al., "On the Overestimation of ^{238}U Resonance Capture by Equivalence Theory," *Proc. Int. Conf. Mathematics and Computational Methods Applied to Nuclear Science and Engineering (M&C 2013)*, Sun Valley, Idaho, May 5–9, 2013, American Nuclear Society (2013).

26. W. ROTHENSTEIN, C. R. E. DE OLIVEIRA, and N. BRANDMAN, "Accurate Resonance Absorption Calculations Including 2-D Effects and Their Representation in Multigroup Lattice Physics Codes," *Ann. Nucl. Energy*, **15**, 293 (1988); http://dx.doi.org/10.1016/0306-4549(88)90093-X.

27. C. C. STOKER and Z. J. WEISS, "Spatially Dependent Resonance Cross Sections in a Fuel Rod," *Ann. Nucl. Energy*, **23**, 765 (1996); http://dx.doi.org/10.1016/0306-4549(95)00074-7.

28. T. SUGIMURA and A. YAMAMOTO, "Evaluation of Dancoff Factors in Complicated Geometry Using the Method of Characteristics," *J. Nucl. Sci. Technol.*, **43**, 1182 (2006); http://dx.doi.org/10.1080/18811248.2006.9711210.

29. F. LESZCZYNSKI, "Neutron Resonance Treatment with Details in Space and Energy for Pin Cells and Rod Clusters," *Ann. Nucl. Energy*, **14**, 589 (1987); http://dx.doi.org/10.1016/0306-4549(87)90094-6.

30. J. ROWLANDS et al., "LWR Pin Cell Benchmark Intercomparisons. An Intercomparison Study Organised by the JEFF Project, with Contributions by Britain, France, Germany, the Netherlands, Slovenia and the USA," JEFF Report 15, Nuclear Energy Agency/Organisation for Economic Co-operation and Development (Sep. 1999).